TISSUE ENGINEERING: Part A
Volume 21, Numbers 15 and 16, 2015

DOI: 10.1089/ten.tea.2014.0484

termis
Tissue Engineering
& Regenerative Medicine
International Society

ORIGINAL ARTICLE

Epigenetically Modified Bone Marrow Stromal Cells in Silk Scaffolds Promote Craniofacial Bone Repair and Wound Healing

Qianqian Han, DDS, PhD,[1–3,*] Pishan Yang, DDS, PhD,[2,4,*] Yuwei Wu, DDS, PhD,[1] Shu Meng, DDS, PhD,[1] Lei Sui, DDS, PhD,[1] Lan Zhang, DDS, PhD,[1] Liming Yu, DDS, MSc,[1] Yin Tang, DDS, PhD,[1] Hua Jiang, DDS, PhD,[1] Dongying Xuan, DDS, PhD,[1,3] David L. Kaplan, PhD,[5] Sung Hoon Kim, PhD,[6] Qisheng Tu, MD, PhD,[1] and Jake Chen, DMD, PhD[1,7]

Epigenetic regulation of gene expression is a central mechanism that governs cell stemness, determination, commitment, and differentiation. It has been recently found that *PHF8*, a major H4K20/H3K9 demethylase, plays a critical role in craniofacial and bone development. In this study, we hypothesize that *PHF8* promotes osteoblastogenesis by epigenetically regulating the expression of a nuclear matrix protein, special AT-rich sequence-binding protein 2 (*SATB2*) that plays pivotal roles in skeletal patterning and osteoblast differentiation. Our results showed that expression levels of *PHF8* and *SATB2* in preosteoblasts and bone marrow stromal cells (BMSCs) increased simultaneously during osteogenic induction. Overexpressing *PHF8* in these cells upregulated the expression of *SATB2*, *Runx2*, osterix, and bone matrix proteins. Conversely, knockdown of *PHF8* reduced the expression of these genes. Furthermore, ChIP assays confirmed that *PHF8* specifically bound to the transcription start site (TSS) of the *SATB2* promoter, and the expression of H3K9me1 at the TSS region of *SATB2* decreased in *PHF8* overexpressed group. Implantation of the BMSCs overexpressing *PHF8* with silk protein scaffolds promoted bone regeneration in critical-sized defects in mouse calvaria. Taken together, our results demonstrated that *PHF8* epigenetically modulates *SATB2* activity, triggering BMSCs osteogenic differentiation and facilitating bone formation and regeneration in biodegradable silk scaffolds.

Introduction

Over 500,000 surgeries correcting bone deformities and critical size defects occur each year, yet 50% of typical graft procedures fail.[1,2] Consequently, the repair of massive bony defects remains challenging in the clinical setting. Tissue engineering provides a new method for bone regeneration. It has three parts: the source of seed cells, suitable scaffold material, and effective cytokines. The ideal scaffold should have good biodegradability, distinguishing mechanical properties, and low inflammatory response. As a natural material, silk scaffold (SS) has good histocompatibility and excellent slow-release function because of its special porous mesh membrane structure. Now, SS, which was used for bone tissue engineering scaffold, has been in the stage of clinical trials. Kim *et al.*[3] used silk nanofiber membrane as scaffold to repair cranial defects and found completely new bone repair after 12 weeks and exhibited no inflammatory response. Our lab also used SSs to repair mouse skull defects and achieved good results.[4–6] Stem cells play pivotal roles in bone tissue regeneration and bone wound repairing. We have previously explored the effects of bone marrow stromal cells (BMSCs) and induced pluripotent stem cells regulated by the osteogenic transcription

[1]Division of Oral Biology, Tufts University School of Dental Medicine, Boston, Massachusetts.
[2]Shandong Provincial Key Lab of Oral Biomedicine, Jinan, China.
[3]Guangdong Provincial Stomatological Hospital, Guangzhou, China.
[4]Department of Periodontology, School of Stomatology, Shandong University, Jinan, China.
[5]Department of Biomedical Engineering, Tufts University, Medford, Massachusetts.
[6]Cancer Preventive Material Development Research Center (CPMDRC) and Institute, College of Oriental Medicine, Kyung Hee University, Seoul, Korea.
[7]Department of Anatomy and Cell Biology, Tufts University School of Medicine, Sackler School of Graduate Biomedical Sciences, Boston, Massachusetts.
*These authors contributed equally to this work.

factors in osteogenetic differentiation and bone regeneration.[5–9] The differentiation of stem cells toward specific functional cell types is the process used to establish specific gene expression patterns, which is a result of elaborated control of activation/silencing of large numbers of genes. Initial regulation in coordinating the expression of osteogenic genes and orchestrating molecular mechanisms in osteoblastogenesis exists and epigenetic regulation of gene expression may serve this role.

Epigenetic modification does not involve changes in DNA sequence, but it causes alterations in DNA methylation and acetylation pattern that modifies the local chromatin structure and thereby serves to regulate expression of specific genes. Histone methylation played important roles in cellular proliferation and differentiation.[10,11] *PHF8* was a histone demethylase associated with X-linked mental retardation. *PHF8* bound through its PHD domain to H3K4me3 nucleosomes and demethylated H3K9, H3K27, and H4K20 at the transcription start site (TSS) regions of active promoters[12,13] and then regulated gene transcription.

PHF8 has been shown to be involved in various biological processes. It has been confirmed that *PHF8* regulates many cell cycle genes[14] and controls the expression of genes associated with cell adhesion and cytoskeleton organization such as RhoA, Rac1, and GSK3β.[15] *PHF8* was also shown to govern retinoic acid response in acute promyelocytic leukemia[16] and affect cell migration and invasion in cancer.[17] Besides, *PHF8* regulates rRNA synthesis via its histone H3K9me1/2 demethylase activity.[18,19]

It has been recently found that *PHF8* played a critical role in craniofacial and bone development.[20] Using a zebrafish model Qi *et al.* found that *PHF8* was mostly expressed in the head and jaw regions. Injection of a *zPHF8* morpholino caused abnormalities in craniofacial organs and wild-type (but not catalytically inactive) *zPHF8* showed significant rescue of craniofacial defects induced by zPHF8 morpholino. These important findings identified a critical role of *zPHF8* in craniofacial development.

Special AT-rich sequence-binding protein 2 (*SATB2*) is a DNA-binding protein that regulates chromatin organization and gene expression.[21] Similar to *PHF8*, *SATB2* is also expressed in branchial arches and osteoblast-lineage cells. *SATB2*$^{-/-}$ mice exhibited defects in osteoblast differentiation and function, which consequently delayed bone formation and mineralization. *SATB2*$^{-/-}$ embryos showed multiple craniofacial defects including a significant truncation of the mandible and a cleft palate.[22] Our previous studies demonstrated that *SATB2* enhanced expressions of bone matrix proteins and osteogenic transcription factors in BMSCs and dental follicle cells, and played pivotal roles in bone regeneration, suggesting that *SATB2* can be used as an osteogenic transcription factor to overcome hurdles in craniofacial regeneration.[9] However, the profiles of the epigenetic regulation of the *SATB2* expression during osteogenic differentiation of BMSCs, particularly in oral and craniofacial development are still largely unknown.

The studies described above indicate the similarities in gene expression and function between *PHF8* and *SATB2*. In this study, we characterized the epigenetic regulation of *PHF8* on *SATB2* in BMSCs and the role of *PHF8* in osteoblast differentiation and calvarial bone regeneration in mouse calvarial defects filled with BMSCs packed in SSs.

Materials and Methods

Cell culture

MC3T3-E1 murine preosteoblast cells were maintained in alpha minimum essential medium (α-MEM) with 10% fetal bovine serum and antibiotics. The MC3T3-E1 cells were then cultured in medium containing 50 mg/mL ascorbic acid (Sigma) and 5 mM β-glycerophosphate (Sigma) to induce osteogenic differentiation. BMSCs were obtained from the femurs and tibias of 4-week-old mice, were cultured in DMEM supplemented with 20% fetal bovine serum and antibiotics in cell culture dish with a diameter of 60 mm (Becton, Dickinson and Company) until they reached 80–90% confluence, and then passaged and maintained at α-MEM supplemented with 10% fetal bovine serum and 1% penicillin/streptomycin as we described previously.[23] To induce osteogenic differentiation of BMSCs, cells were switched to osteogenic medium containing 50 mg/mL ascorbic acid (Sigma), 10 nM dexamethasone (Sigma), and 5 mM β-glycerophosphate (Sigma) for 1, 3, 7, 10, 14, and 21 days, respectively.

Preparation of retroviral vectors and cell infection

The plasmids pBABE-control shRNA, pBABE-*PHF8* shRNA, and pOZ-Flag-HA-*PHF8* (mouse *PHF8* cDNA) were a generous gift from Dr. Yang Shi's laboratory (Department of Pathology, Harvard Medical School). The pOZ-Flag-HA-*PHF8* and packaging vectors pOZ-ENV and pOZ-Gagpol were co-transfected into HEK-293T cells using lipofectamine 2000 (Invitrogen). Forty-eight hours after transfection, the supernatant filtered through a 0.45 mm filter (Millipore) was used to infect targeted cells with polybrene at a final concentration of 8 μg/mL. The empty retroviral vector pOZ-Flag-HA was also packaged and used as a control. pBABE-*PHF8* shRNA and packing vector pCG-Gagpol and pCG-VSVG were co-transfected into HEK-293T cells to construct the viruses expressing *PHF8* shRNA. Quantitative reverse transcription polymerase chain reaction (RT-PCR) assay was used for quantification of both genomic viral RNA after production and of targeted gene transcripts following transduction.

Cytoimmunofluorescence test

The glass coverslips were put in 24-well plate and the MC3T3-E1 cells were seeded in 24-well plate. The following day, cells were fixed with 4% paraformaldehyde, followed by permeabilization with 0.05% Triton X-100 (Sigma-Aldrich). Then, cells were blocked for 30 min with 10% normal donkey serum and incubated with *PHF8* primary antibody (Abacm) overnight at 4°C. After three washes of 5 min each in phosphate-buffered saline (PBS), the cells were incubated in conjugated secondary antibody (Alexa 488 green; Invitrogen) and then mounted with ProLong® Gold Antifade Reagent with DAPI (Invitrogen). Images were collected using an Axiovert 405 M epifluorescence inverted light microscope (Lumen200; Prior Scientific, Inc.) and an Olympus DP 73 digital camera.

Real-time RT-PCR for mRNA analysis

Real-time *RT-PCR* for mRNA analysis was performed using SYBR Green Mastermix (Affymetrix) on a Bio-Rad iQ5 thermal cycler (Bio-Rad Laboratories). The relative expression

level of the housekeeping gene GAPDH was used to normalize gene expression in each sample in different groups. The sequences of the primer for amplification of mouse ALP, BSP, OCN, *Runx2*, osterix, *SATB2*, *PHF8*, and GAPDH were shown in Supplementary Table S1 (Supplementary Data are available online at www.liebertpub.com/tea).

Western blot analysis

MC3T3-E1 and BMSCs were infected with viruses that express *PHF8*, empty vector, *PHF8* shRNA, and control shRNA, respectively. Whole protein lysates were prepared as described previously.[24] Antibodies for *PHF8* (Abcam), *SATB2*, OSX, and *Runx2* were obtained from Santa Cruz Biotechnologies. The second antibody was HRP-labeled goat anti-rabbit IgG (Santa Cruz). The proteins were visualized using electrogenerated chemiluminescence reagents from Pierce Biotechnology. Image J was used to qualify the protein expression.

ChIP analysis

The MC3T3-E1 cells and BMSCs from a 150 cm plate were cross-linked with 10% formaldehyde and quenched with 0.125 M glycine. Cells were washed with cold PBS and then lysed with cell lysis buffer complemented with protease inhibitor Cocktail II (Sigma). DNA fragmentation was performed with Vibra-Cell™ sonicator using 500 μL nuclear lysis buffer lysate with 20 cycles of 15 s ON and 45 s OFF. In qChIP, 100 μg of chromatin were incubated with 2 μg of *PHF8* antibody (Abcam) or 2 μg of the H3K9me1 antibody (Abcam) at 4°C overnight. Twenty microliters of Protein A or G beads was added to each tube for 2 h at 4°C and the complex were then washed with low salt buffer, high salt buffer, LiCl buffer, and TE buffer each for 5 min. The immunoprecipitants were de-cross-linked at 62°C overnight. The immunoprecipitated DNA was dissolved in 30 μL H_2O. One microliter of DNA was used for real-time polymerase chain reaction (PCR). The primers for qChIP were shown in Supplementary Table S2.

SS preparation and cell seeding

The silk fibroin scaffolds (disk-shaped, 4 mm diameter and 2 mm thick) were prepared as described previously.[5,25] For cell seeding, cells were released from the culture substratum and concentrated to 2×10^7 cells/mL in serum-free medium. Then, BMSCs were seeded into the SSs by pipetting 0.5 mL of the cell suspension onto the materials. The BMSCs/SS construct was incubated overnight to allow cell attachment *in vitro* before implantation.

Animal surgery

The animal protocols used in this study were approved by the Institutional Animal Care and Use Committee at Tufts University/Tufts Medical Center (Approved Protocol #B2011-49). All mice were kept in a controlled temperature- and controlled room under a 12 h light, 12 h dark cycle.

Eight-week-old C57BL/6J mice were anesthetized, and a 4-mm-diameter calvarial critical-sized defect was created on each side of the calvarial bone using a dental bur attached to a slow-speed hand piece with minimal invasion of the Dura mater. The critical-sized defects in mice were randomly divided into six groups to receive the following implants ($n = 5$ per group): (1) SS alone; (2) SS with BMSCs; (3) SS with *PHF8*-modified BMSCs; (4) SS with empty vector-modified BMSCs; (5) SS with *PHF8* shRNA-modified BMSCs; (6) SS with control shRNA-modified BMSCs.

Quantitative real time reverse transcription polymerase chain reaction of newly formed tissue

The mice were sacrificed 5 weeks after surgery and the newly formed bone samples were frozen immediately in liquid nitrogen. Total RNA was extracted using TRIzol reagent (Invitrogen) from the newly formed tissues and used for cDNA synthesis. Real-time PCR was used to detect the mRNA expressions of ALP, BSP, OCN, *SATB2*, *Runx2*, OSX, and *PHF8*.

Micro CT measurement

Five weeks after surgery, the morphology of the reconstructed cranium was assessed using a micro-CT system (μCT-40; Scanco Medical). The CT settings were used as follows: pixel matrix, 1024×1024; slice thickness, 20 mm. After scanning, the micro-CT images were segmented using a nominal threshold value of 300 as reported previously[5] and a three dimensional histomorphometric analysis was performed automatically. The parameters of bone volume were used for comparison in this study.

Histomorphometric analysis and immunohistochemical staining

For histological examination, cranial specimens were fixed with 10% formalin and then decalcified with 10% ethylenediaminetetraacetic acid (pH 7.0) for 2 weeks. Samples were then dehydrated in ethanol and embedded in paraffin wax. Five-millimeter sections were cut and mounted on glass slides. Three randomly selected sections from each sample were stained with hematoxylin and eosin (H&E). H&E staining was performed using standard methods as previously described.[26] The expressions of OCN were detected using immunohistochemical staining followed by counterstaining in hematoxylin with a Histostain SP kit (Invitrogen). H&E staining and immunostaining sections were photographed with an OLYMPUS BX53 microscope. Newly formed bone in H&E-stained sections was quantified in five sections of at least five different defects for each treatment at 200× magnification using Image Pro Plus software. New bone formation on each section was expressed as a percentage of the total area of the defect. The localization of OCN staining was studied on transverse sections of the cranium as previously described.[26] All slides were coded to prevent the introduction of examiner bias.

Long bones, calvarial bone, periodontal ligament, heart, brain, kidney, liver, and muscle tissues were also collected from 8-week wild-type mice without surgery. Five-millimeter sections were cut and mounted on glass slides. The expressions of *PHF8* were detected using immunohistochemical staining followed by counterstaining in hematoxylin with a Histostain SP kit (Invitrogen).

Statistical analysis

All results were expressed as mean ± standard error of the mean of three or more independent experiments. One-way analysis of variance with *post-hoc* tests was used to test significance using the software SPSS 13.0. Values of $p < 0.05$ were considered statistically significant.

Results

The cellular localization of PHF8 *and the expression pattern of* PHF8 *in different tissues*

To detect the expression pattern of *PHF8* in different tissues, we collected tissues from 8-week wild-type mice and used immunohistochemical staining to detect the *PHF8* expression (Fig. 1A–I). We found that there was little *PHF8* expression in kidney, liver, and muscle. In heart, only a few cells were *PHF8*-positive cells. In long bones, calvarial bones, and periodontal ligaments, there were more *PHF8*-positive cells than that in other tissues. Importantly, the *PHF8*-positive cells mainly distributed in the growth plate of long bone and the cranial suture. These results indicated that *PHF8* might play an important role in bone formation and regeneration.

PHF8 is a histone demethylase and it exhibits its demethylase activity in the nucleus. In this study, we used immunocytofluorescent staining to detect the cellular localization of *PHF8* and found that *PHF8* expressions were localized in nucleus in MC3T3-E1 cells (Fig. 1J).

The expression of PHF8 increased during osteogenic differentiation

BMSCs were obtained from 4-week-old mice and treated with osteogenic medium for 1, 3, 7, 10, 14, and 21 days, respectively. RNA was extracted and real-time PCR was conducted to detect the gene expression of *PHF8*. Our results showed that the expression of both *PHF8* and *SATB2* increased during osteogenic differentiation (Fig. 2A).

PHF8 promoted osteogenic differentiation of MC3T3-E1 cells and BMSCs

To determine whether *PHF8* affects osteogenic differentiation, we overexpressed or knocked down *PHF8* expression in MC3T3-E1 cells and BMSCs. The results showed that *PHF8* overexpression upregulated the expression of all bone marker genes and knockdown of *PHF8* using shRNA downregulated the expression of *SATB2*, OSX, *Runx2*, BSP, and OC in MC3T3-E1 cells and BMSCs (Figs. 2B, C and 3). These results provided the evidence that *PHF8* promoted osteogenic differentiation of MC3T3-E1 cells and BMSCs.

PHF8 directly bound to the TSS region of SATB2

To detect the mechanism of how PHF8 regulates osteogenic differentiation, we performed ChIP analysis to determine whether *PHF8* can directly bind to transcription factor *SATB2*. MC3T3-E1 cells were treated with osteogenic medium for 7 and 14 days, and then cross-linked. The DNA-protein complex was then incubated with *PHF8* antibody

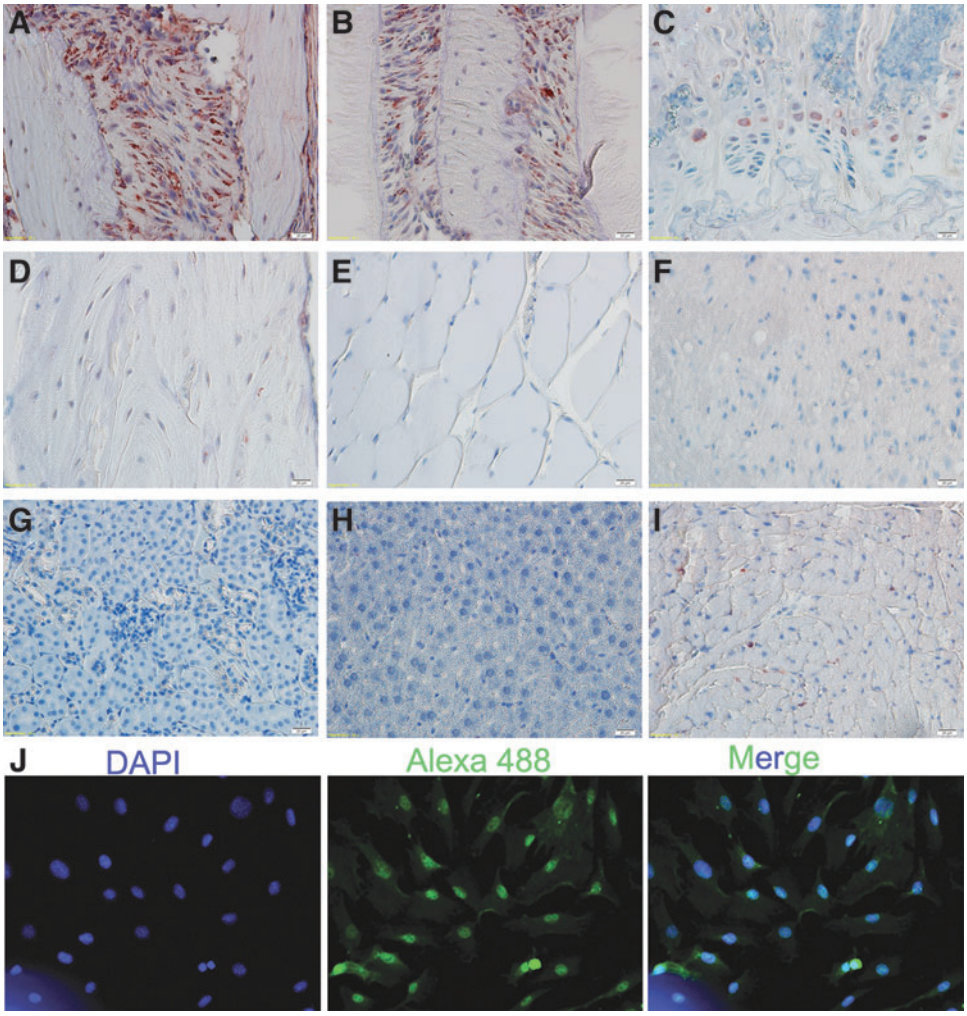

FIG. 1. The localization of PHF8 and the expression pattern of *PHF8* during osteogenic differentiation. Original magnification: 400×. **(A–I)** The expression pattern of *PHF8* in different tissues detected by IHC. **(A)** Calvarial bone; **(B)** periodontal ligament; **(C)** growth plate; **(D)** long bone; **(E)** muscle; **(F)** brain; **(G)** kidney; **(H)** liver; **(I)** heart; **(J)** The cellular localization of *PHF8*. *PHF8* protein was labeled with Alexa 488 green, and nuclei were labeled with DAPI (*blue*). Color images available online at www.liebertpub.com/tea

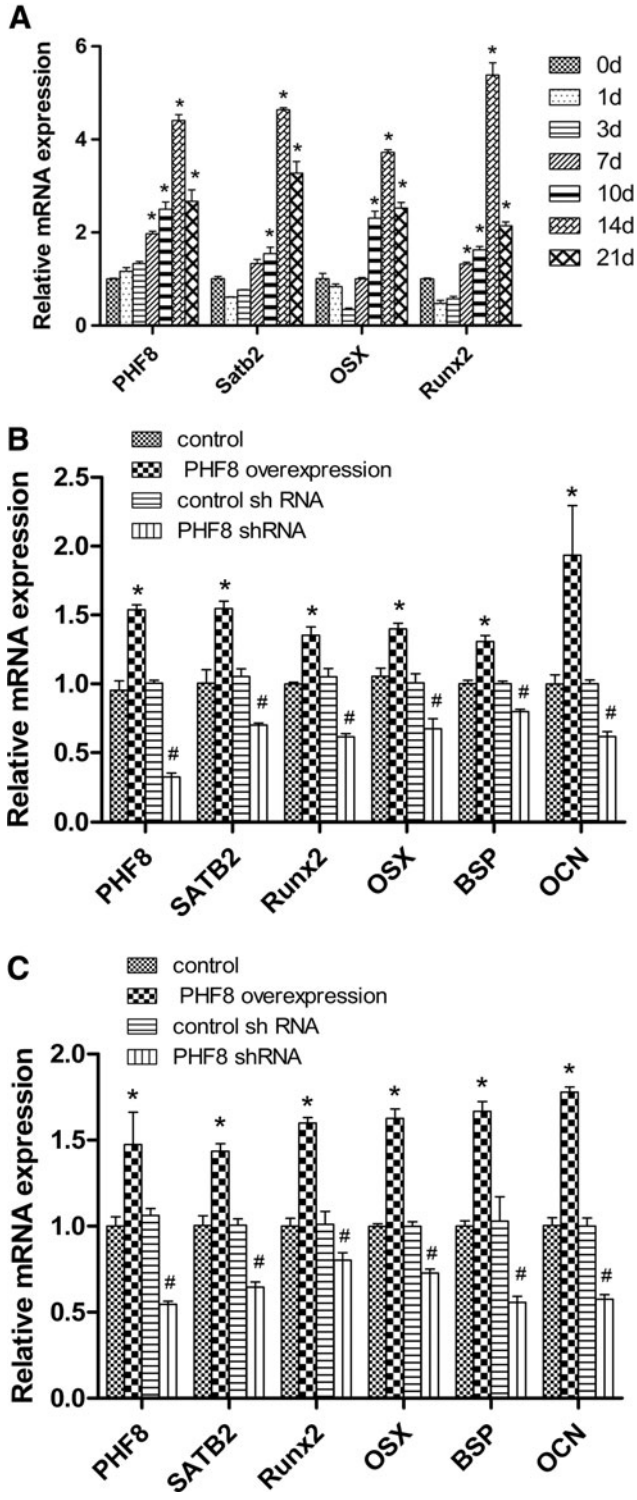

FIG. 2. *PHF8* regulated the gene expression levels of the osteogenic markers. The expression of *PHF8*, *SATB2*, OSX, and *Runx2* increased during osteogenic differentiation, $^{*}p < 0.05$ versus 0 day group **(A)**. *PHF8* cDNA overexpression and knockdown of *PHF8* using shRNA, respectively, in MC3T3-E1 cells **(B)** and BMSCs **(C)**. The gene expressions of *SATB2*, OSX, *Runx2*, BSP, and OCN were detected by realtime reverse transcription polymerase chain reaction. $^{*}p < 0.05$ versus control vector group; $^{\#}p < 0.05$ versus control shRNA group. BMSCs, bone marrow stromal cells; *SATB2*, special AT-rich sequence-binding protein 2.

and then DNA was extracted. The results showed that *PHF8* bound to the TSS region of *SATB2* gene (Fig. 4A). We also found that the binding of *PHF8* to the TSS region of *SATB2* increased when cells were treated with osteogenic medium (Fig. 4A).

PHF8 regulated osteogenic differentiation via demethylating H3K9me1 at the promoter of SATB2

To determine whether *PHF8* regulates *SATB2* transcription through the H3K9me1 demethylase activity, we overexpressed or knocked down *PHF8* expression in MC3T3-E1 cells undergoing osteogenic differentiation, and then performed ChIP analysis to detect the binding of H3K9me1 at the promoter of *SATB2*. Our results confirmed that overexpressing *PHF8* downregulated the binding of H3K9me1 at the TSS region of *SATB2*, while knockdown of *PHF8* using shRNA upregulated the binding of H3K9me1 (Fig. 4B, C). H3K9me1 can silence gene transcription and the demethylation of H3K9me1 causes the DNA to unwind from histone protein, and converting chromatin into a transcriptionally active conformation. Therefore, this result suggested that the binding of *PHF8* to *SATB2* and the resultant demethylation activity of *PHF8* toward H3K9me1 at the promoter of *SATB2* converted *SATB2* into a transcriptional active conformation.

Enhancement of bone healing by transduction of PHF8 in mice

Critical size full thickness defects of 4 mm in diameter were made in both sides of the cranial bone and filled with a SS seeded with gene-modified BMSCs. Five weeks after surgery, micro CT was used to detect the morphology of the newly formed bone and evaluate new bone formation within the defects. As shown in Figure 5, larger, newly formed bone filled the defects of the *PHF8*-modified BMSCs group when compared with the empty vector-modified or unmodified groups, which showed the formation of scattered new bone in the defect sites (Fig. 5A). No obvious evidence of new bone formation was observed in the defects filled with scaffolds alone or *PHF8* shRNA-modified BMSCs (Fig. 5A).

To quantify the new bone regeneration within the calvarial defects, the volume of regenerated bone (BV) were measured. As shown in Figure 5C, BV was significantly higher for the *PHF8*-modified BMSCs group when compared with all other groups. Histological evidence further supported the micro CT results, indicating that the specimens from the *PHF8*-modified BMSCs group showed the most extensive new bone formation (Fig. 5B). In contrast, a small amount of newly formed bone tissue was shown in the empty vector-modified BMSCs, unmodified BMSCs group, or control shRNA-modified group. Defects were filled with fibrous connective tissue and no obvious bone formation was found in the *PHF8* shRNA-modified BMSCs group and scaffold alone group (Fig. 5B). The percentage of new bone area in the *PHF8*-modified BMSCs group was significantly higher than the other four groups 5 weeks postoperation (Fig. 5D). To further analyze the new bone mineralization, immunohistochemistry was performed to determine OCN expression levels. As shown in Figure 6, immunohistochemistry exhibited strong expression for OCN in areas of new bone formation within the defect region from samples

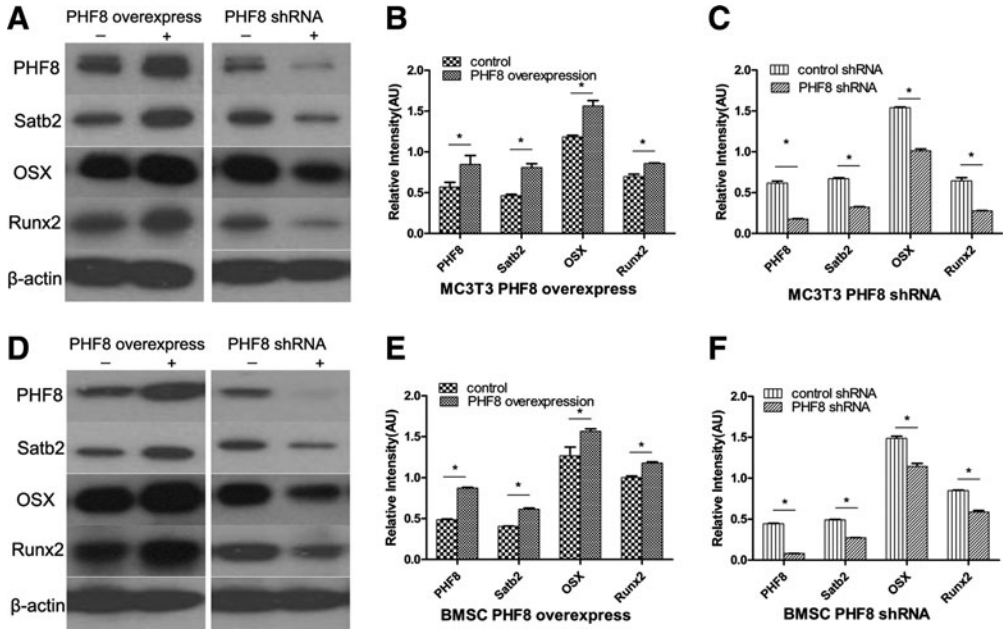

FIG. 3. *PHF8* regulated bone transcription factors. The protein expressions of *PHF8*, Satb2, OSX, and *Runx2* were detected by western blot. **(A)** *PHF8* overexpression (*left panel*) and *PHF8* suppression by shRNA (*right panel*) in MC3T3-E1 cells. **(B, C)** Quantification of protein levels. **(D–F)** The same experiments as **(A–C)** in BMSCs. $*p < 0.05$.

treated with the *PHF8*-modified BMSCs, whereas OCN staining was weaker in empty vector-transduced BMSCs, control shRNA-modified BMSCs, and untransduced BMSCs groups. Moreover, no obvious positive staining was observed in the *PHF8* shRNA-modified BMSCs group or scaffold alone group (Fig. 6A–F). Moreover, to further determine the effect of *PHF8*-modified BMSCs in new bone formation, total RNA was isolated from four the experimental groups (*PHF8*-modified BMSCs group; empty vector-modified BMSCs group; *PHF8* shRNA-modified BMSCs group; control shRNA-modified BMSCs group), and quantitative real time reverse transcription polymerase chain reaction was performed to detect mRNA expression levels of ALP, BSP, OCN, SATB2, *Runx2*, and OSX. As shown in Figure 6, the ALP, BSP, OCN, *SATB2*, *Runx2*, and OSX mRNA expression showed a higher level in the defects with *PHF8*-modified BMSCs group than the control group 5 weeks postoperation (Fig. 6G), while knockdown of *PHF8* expression using shRNA in BMSCs inhibited the expression of these genes (Fig. 6H). These results demonstrated that BMSCs modified with *PHF8* and seeded on SSs enhanced cranial critical-size bone healing in mice.

Discussion

Epigenetic regulation has been shown to play an important role in various biological processes. As one of the modes of epigenetic regulation and a mechanism for modifying

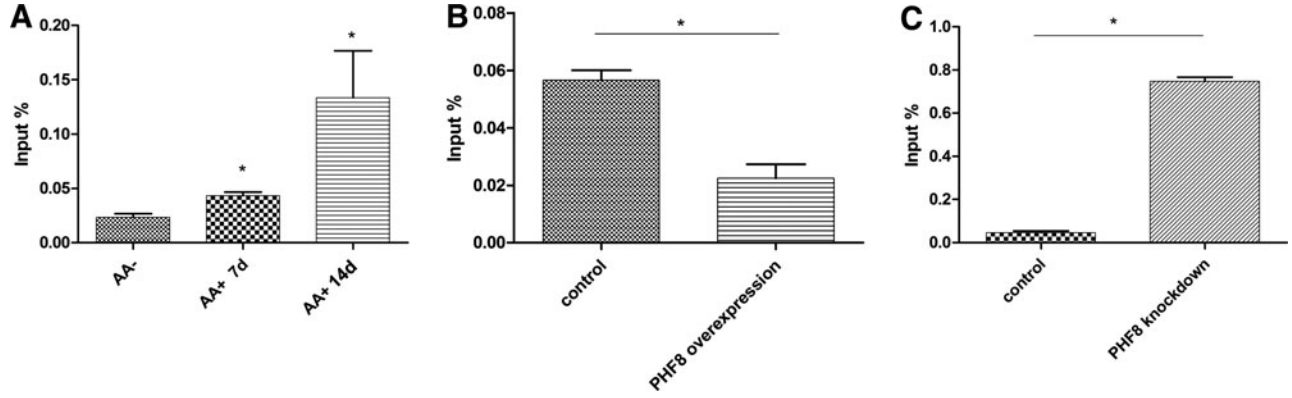

FIG. 4. ChIP-qPCR analyze the binding of *PHF8* and H3K9me1 on Satb2. **(A)** MC3T3-E1 cells were treated with osteogenic medium for 7 and 14 days, and then cross-linked. The DNA-protein complex was then incubated with *PHF8* antibody and then DNA was extracted, real-time PCR was used to detect the binding of *PHF8* on SATB2. **(B, C)** *PHF8* was overexpressed **(B)** or suppressed **(C)** in MC3T3-E1 cells, and then cross-linked. The DNA-protein complex was incubated with H3K9me1 antibody and then DNA was extracted, real-time PCR was used to detect the binding of H3K9me1 on *SATB2*. $*p < 0.05$. PCR, polymerase chain reaction.

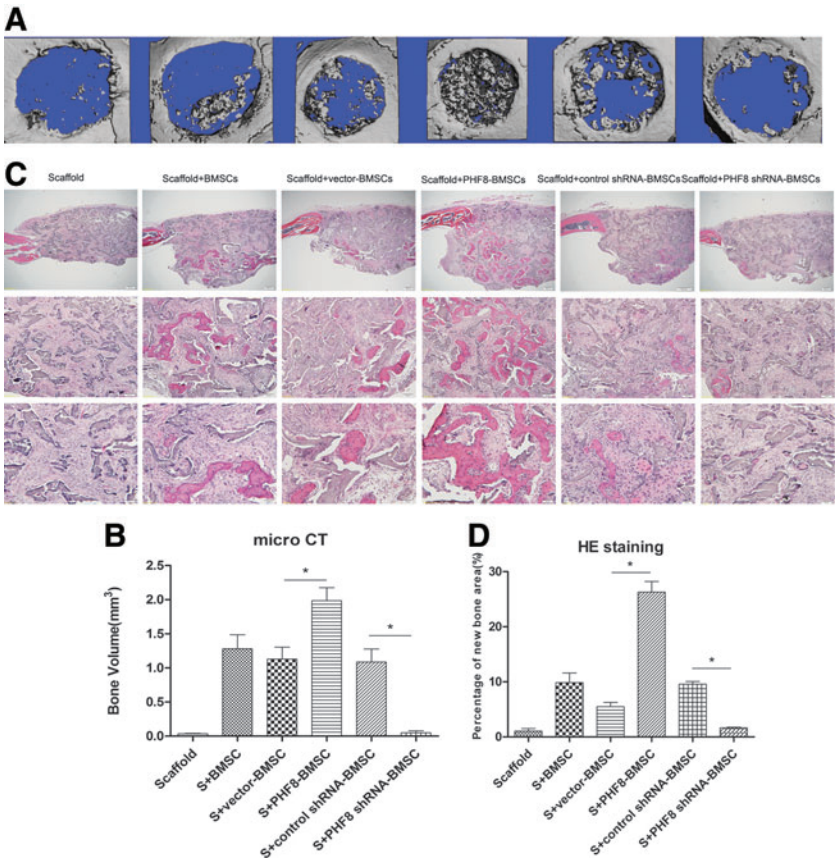

FIG. 5. Micro CT and HE staining analysis. **(A)** Five weeks after surgery, micro CT results indicated the *PHF8*-modified BMSCs group showed the largest amounts of new bone formation. **(B)** HE staining demonstrated that *PHF8*-modified BMSCs group showed more new bone formation than other groups. Original magnification: *top panel*, 40×; *middle panel*, 200×; *bottom panel*, 400×. **(C)** Volume of newly formed bone detected by micro CT. **(D)** Percentage of new bone area in different treatment groups measured in HE staining sections. HE, hematoxylin and eosin; S, scaffold; $*p < 0.05$. Color images available online at www.liebertpub.com/tea

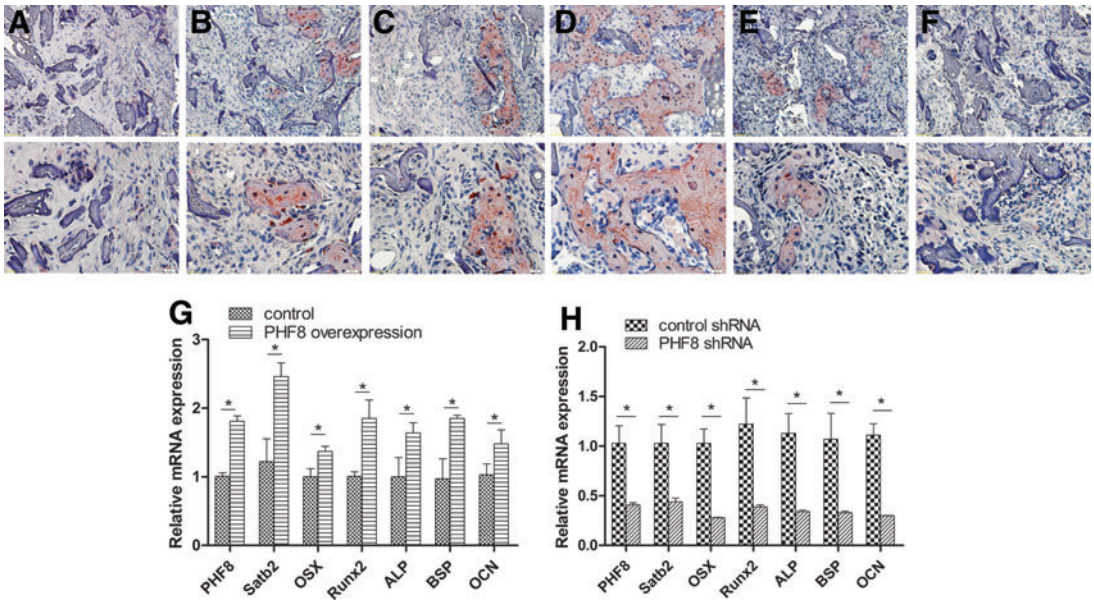

FIG. 6. Immunohistochemical and real-time PCR analysis of newly formed bones. **(A–F)** Immunohistochemical analysis of new bone formation in each group at 5 weeks postoperation **(A–F)**; Original magnification: *upper panel*, 200×; *lower panel*, 400×). OCN staining demonstrates no obvious positive staining in scaffold alone **(A)** and *PHF8* shRNA-modified BMSCs group **(F)**, while a weak OCN staining in scaffold with BMSCs group **(B)**, vector-modified BMSCs group **(C)** and control shRNA-modified BMSCs group **(E)**, and a stronger OCN expression was observed in the new bone tissue from *PHF8*-modified BMSCs group **(D)**. **(G–H)** Gene expression levels of *PHF8*, Satb2, ALP, OSX, *Runx2*, OCN, and BSP in the new bone of *PHF8*-modified BMSCs treatment group **(G)** and *PHF8* shRNA treatment group **(H)**. $*p < 0.05$. Color images available online at www.liebertpub.com/tea

chromatin structure, histone methylation was associated with the stimulation of several pathways known to be important for biological processes including neural development,[27] vascular development,[28,29] and bone regeneration.[30,31] Our research aimed to characterize the role *PHF8* played in osteogenic differentiation and bone regeneration.

In this study, we first detected the distribution of the PHF8 in different tissues in mice. We found that there were more *PHF8*-positive cells in the growth plate of the long bone and calvarial sutures than other tissues in 8-week mice. The growth plate is responsible for bone lengthening[32] and sutures play an important role in bone repair and bone regeneration.[33] Based on the distribution of *PHF8* expression in these tissues, we hypothesized that *PHF8* plays an important role in bone regeneration. When we treated BMSCs and preosteoblasts with osteogenic medium, we found that the gene expression of *PHF8* and other osteogenic markers such as *SATB2*, *Runx2*, and OSX were upregulated compared with control groups. These results indicated that *PHF8* might play an important role in osteogenic differentiation of BMSCs and MC3T3-E1.

BMSCs can differentiate into several kinds of cells including osteoblasts and play an important role in bone regeneration.[34,35] Enhanced osteogenic differentiation of BMSCs induced by genetic modification could change the character of these cells. Such genetic modifications were frequently achieved by overexpression of regulatory proteins such as BMP2 and VEGF.[36,37] In this study, we found that *PHF8* overexpression increased the expression of *SATB2*, *Runx2*, OSX, ALP, BSP, and OCN while knockdown of *PHF8* downregulated the expression of those genes in MC3T3-E1 cells and BMSCs. Our previous studies and those of other labs confirmed that *SATB2* plays an important role in osteogenic differentiation and bone regeneration,[5,38] and *SATB2* regulates the expression of OSX during osteoblast differentiation.[9] Given that *SATB2* plays an important role in integrating genetic and epigenetic signaling[39] and *PHF8* overexpression upregulated the expression of *SATB2* during osteogenic differentiation, we inferred that *PHF8* might regulate SABT2 to activate osteogenic differentiation of BMSCs. To this end, we performed ChIP analysis to confirm the epigenetic regulation of *PHF8* through *SATB2*.

Epigenetic regulation is largely controlled by histone modifications, which enable gene promoters to be accessible or inaccessible to transcription factors.[40,41] One such important histone modification is histone H3 lysine monomethylation (H3K9me1) on gene promoters, which silences gene transcription.[42] *PHF8* is a histone demethylase that can demethylate H3K20 and H3K9me1/2,[19] and it apparently would be localized in the nucleus of the cells. We first confirmed that *PHF8* was mainly localized in the nucleus of the cells using immunocytofluorescent assays. Then, ChIP analysis found that PHF8 bound to the TSS region of *SATB2*. More interestingly, the occupancy of the PHF8 at the TSS region increased during osteogenic differentiation. These results indicated that PHF8 might promote osteogenic differentiation via regulation the expression of *SATB2*. Next, we performed another ChIP analysis and found that PHF8 overexpression decreased the binding of H3K9me1 to the promoter of *SATB2*. As PHF8 is an H3K9me1/2 demethylase, these results indicated that PHF8 could demethylate H3K9me1 at the promoter region of *SATB2*, thus causing the DNA to unwind from histone protein, and converting *SATB2* into a transcriptionally active conformation. These *in vitro* data confirmed that PHF8 regulated the expression of *SATB2* via its histone demethylation activity and then promoted osteogenic differentiation.

Tissue engineering has been widely used in bone research field, which is an especially good choice to repair large size bone defects by using resorbable scaffolds supplemented with regeneration-competent cells and growth factors.[43] The biodegradability, distinguishing mechanical properties, and low inflammatory response of silk fibroin make it a promising scaffold for bone regeneration.[6,44] Our previous research also found that silk fibroin was an ideal scaffold for bone repair.[4,5] As a result, we choose silk fibroin as scaffolds in this research. Besides the scaffolds, the seeded cells and growth factors are key elements for forming tissue-engineered bone. As an important regulator, epigenetic pathways are able to play a crucial role in the control of gene activity during different stages of development and throughout life, which will lead to more effective ways to

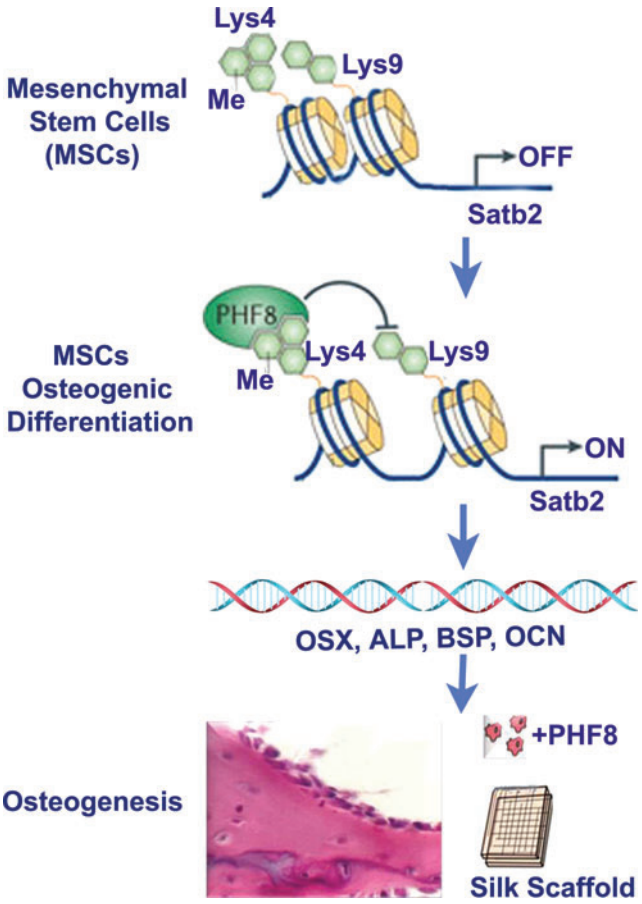

FIG. 7. Schematic representation of epigenetic regulation by *PHF8* in promoting BMSCs osteogenic differentiation and bone repair. *PHF8* demethylate H3K9me1 at the promoter of *SATB2* and activate *SATB2* transcription. *SATB2* then upregulate the expression of osteogenic factors such as OSX, ALP, BSP, OCN, and promote osteogenic differentiation of BMSCs and bone repair. Color images available online at www.liebertpub.com/tea

prevent and treat diseases affecting the oral and craniofacial region. *PHF8* could demethylate H3K9me1 at the promoter of *SATB2* and then promoted osteogenic differentiation *in vitro*. Therefore, we wanted to know whether *PHF8* could promote bone healing *in vivo*. Critical size calvarial bone defects were formed in mice and then implanted with *PHF8*-modified BMSCs in the defects housed within the SSs. We found little new bone formation in the defects 2 weeks after surgery. However, when we used immunohistochemistry to detect the expression of OCN in cells in the defects, we found that there were more OCN-positive cells in *PHF8*-modified BMSCs implanted group (data not shown). These results indicated that *PHF8* could promote osteogenic differentiation of BMSCs *in vivo*. Five weeks after surgery, we found substantially more new bone formation in *PHF8*-modified BMSCs group than other groups. However, little new bone was found in *PHF8* shRNA-modified BMSCs treatment group. These results provided the evidence that *PHF8* played an important role in bone-related wound healing. As an epigenetic regulator, *PHF8* could demethylate H3K9me1 and converted *SATB2* chromatin into a transcriptionally active conformation during osteogenic differentiation. We and other researchers have also shown that *SATB2* acted as a ''node'' to transcriptionally regulate oral and craniofacial development and osteoblast differentiation, and promote bone tissue regeneration.[5,9,38] *PHF8* could be used as a useful epigenetic regulator in the tissue engineering field as it can promote BMSCs osteogenic differentiation and bone regeneration (Fig. 7). Further understanding of how the nuclear matrix gene *SATB2*, chromatin structure modifier *PHF8*, and transcriptional activity coordinate the regulation of multiple steps during osteoblastic differentiation of BMSCs will allow us to better optimize tissue regeneration strategies.

Conclusions

The data demonstrated that *PHF8*, an epigenetic modifier, regulated osteogenic differentiation of BMSCs via modulating H3K9me1 methylation of the master gene *SATB2*. *Ex vivo* gene therapy of *PHF8*-modified BMSCs within SSs effectively promoted bone regeneration in critical-sized calvarial defects. Although further studies are needed to optimize *PHF8* levels during bone regeneration, the present results provide strong evidence for using *PHF8* to repair bone defects.

Acknowledgments

We thank Jean Tang for her assistance in tissue sample preparation and histology, and Dana Murray for her help in the preparation of the article. We are grateful to the other members of the Chen lab for discussion and technical help. This project was supported by National Institutes of Health (NIH) grants R01DE16710 and R01DE21464, and the International Association of Dental Research (IADR) and the Academy of Osseointegration (AO) Innovation in Implant Science Award (to J.C.); Ministry of Education, Science and Technology (MEST) grant 2007-0054931 in South Korea (to S.H.K.); NIH contract grant P41 EB002520 (to D.L.K.).

Disclosure Statement

No competing financial interests exist.

References

1. Boyce, T., Edwards, J., and Scarborough, N. Allograft bone. The influence of processing on safety and performance. Orthop Clin North Am **30,** 571, 1999.
2. Huang, C., Das, A., Barker, D., Tholpady, S., Wang, T., Cui, Q., *et al.* Local delivery of FTY720 accelerates cranial allograft incorporation and bone formation. Cell Tissue Res **347,** 553, 2012.
3. Kim, K.H., Jeong, L., Park, H.N., Shin, S.Y., Park, W.H., Lee, S.C., *et al.* Biological efficacy of silk fibroin nanofiber membranes for guided bone regeneration. J Biotechnol **120,** 327, 2005.
4. Karageorgiou, V., Tomkins, M., Fajardo, R., Meinel, L., Snyder, B., Wade, K., *et al.* Porous silk fibroin 3-D scaffolds for delivery of bone morphogenetic protein-2 in vitro and in vivo. J Biomed Mater Res A **78,** 324, 2006.
5. Ye, J.H., Xu, Y.J., Gao, J., Yan, S.G., Zhao, J., Tu, Q., *et al.* Critical-size calvarial bone defects healing in a mouse model with silk scaffolds and SATB2-modified iPSCs. Biomaterials **32,** 5065, 2011.
6. Jiang, X., Zhao, J., Wang, S., Sun, X., Zhang, X., Chen, J., *et al.* Mandibular repair in rats with premineralized silk scaffolds and BMP-2-modified bMSCs. Biomaterials **30,** 4522, 2009.
7. Xu, B., Zhang, J., Brewer, E., Tu, Q., Yu, L., Tang, J., *et al.* Osterix enhances BMSC-associated osseointegration of implants. J Dent Res **88,** 1003, 2009.
8. Tu, Q., Zhang, J., James, L., Dickson, J., Tang, J., Yang, P., *et al.* Cbfa1/Runx2-deficiency delays bone wound healing and locally delivered Cbfa1/Runx2 promotes bone repair in animal models. Wound Repair Regen **15,** 404, 2007.
9. Zhang, J., Tu, Q., Grosschedl, R., Kim, M.S., Griffin, T., Drissi, H., *et al.* Roles of SATB2 in osteogenic differentiation and bone regeneration. Tissue Eng Part A **17,** 1767, 2011.
10. Zhang, Y., and Reinberg, D. Transcription regulation by histone methylation: interplay between different covalent modifications of the core histone tails. Genes Dev **15,** 2343, 2001.
11. Klose, R.J., Kallin, E.M., and Zhang, Y. JmjC-domain-containing proteins and histone demethylation. Nat Rev Genet **7,** 715, 2006.
12. Kleine-Kohlbrecher, D., Christensen, J., Vandamme, J., Abarrategui, I., Bak, M., Tommerup, N., *et al.* A functional link between the histone demethylase PHF8 and the transcription factor ZNF711 in X-linked mental retardation. Mol Cell **38,** 165, 2010.
13. Horton, J.R., Upadhyay, A.K., Qi, H.H., Zhang, X., Shi, Y., and Cheng, X. Enzymatic and structural insights for substrate specificity of a family of jumonji histone lysine demethylases. Nat Struct Mol Biol **17,** 38, 2010.
14. Lim, H.J., Dimova, N.V., Tan, M.K., Sigoillot, F.D., King, R.W., and Shi, Y. The G2-M regulator, histone demethylase PHF8, is targeted for degradation by APCcdc20. Mol Cell Biol **33,** 4166, 2013.
15. Asensio-Juan, E., Gallego, C., and Martinez-Balbas, M.A. The histone demethylase PHF8 is essential for cytoskeleton dynamics. Nucleic Acids Res **40,** 9429, 2012.
16. Arteaga, M.F., Mikesch, J.H., Qiu, J., Christensen, J., Helin, K., Kogan, S.C., *et al.* The histone demethylase PHF8 governs retinoic acid response in acute promyelocytic leukemia. Cancer Cell **23,** 376, 2013.
17. Bjorkman, M., Ostling, P., Harma, V., Virtanen, J., Mpindi, J.P., Rantala, J., *et al.* Systematic knockdown of epigenetic enzymes identifies a novel histone demethylase PHF8

overexpressed in prostate cancer with an impact on cell proliferation, migration and invasion. Oncogene **31,** 3444, 2012.
18. Zhu, Z., Wang, Y., Li, X., Xu, L., Wang, X., Sun, T., *et al.* PHF8 is a histone H3K9me2 demethylase regulating rRNA synthesis. Cell Res **20,** 794, 2010.
19. Feng, W., Yonezawa, M., Ye, J., Jenuwein, T., and Grummt, I. PHF8 activates transcription of rRNA genes through H3K4me3 binding and H3K9me1/2 demethylation. Nat Struct Mol Biol **17,** 445, 2010.
20. Qi, H.H., Sarkissian, M., Hu, G.Q., Wang, Z., Bhattacharjee, A., Gordon, D.B., *et al.* Histone H4K20/H3K9 demethylase PHF8 regulates zebrafish brain and craniofacial development. Nature **466,** 503, 2010.
21. Alcamo, E.A., Chirivella, L., Dautzenberg, M., Dobreva, G., Farinas, I., Grosschedl, R., *et al.* Satb2 regulates callosal projection neuron identity in the developing cerebral cortex. Neuron **57,** 364, 2008.
22. Dobreva, G., Chahrour, M., Dautzenberg, M., Chirivella, L., Kanzler, B., Farinas, I., *et al.* SATB2 is a multifunctional determinant of craniofacial patterning and osteoblast differentiation. Cell **125,** 971, 2006.
23. Yu, L., Tu, Q., Han, Q., Zhang, L., Sui, L., Zheng, L., *et al.* Adiponectin regulates bone marrow mesenchymal stem cell niche through a unique signal transduction pathway: an approach for treating bone disease in diabetes. Stem Cells **33,** 240, 2015.
24. Valverde, P., Tu, Q., and Chen, J. BSP and RANKL induce osteoclastogenesis and bone resorption synergistically. J Bone Miner Res **20,** 1669, 2005.
25. Kim, H.J., Kim, U.J., Kim, H.S., Li, C., Wada, M., Leisk, G.G., *et al.* Bone tissue engineering with premineralized silk scaffolds. Bone **42,** 1226, 2008.
26. Tu, Q., Valverde, P., Li, S., Zhang, J., Yang, P., and Chen, J. Osterix overexpression in mesenchymal stem cells stimulates healing of critical-sized defects in murine calvarial bone. Tissue Eng **13,** 2431, 2007.
27. Zovkic, I.B., and Sweatt, J.D. Epigenetic mechanisms in learned fear: implications for PTSD. Neuropsychopharmacology **38,** 77, 2013.
28. Villeneuve, L.M., Reddy, M.A., Lanting, L.L., Wang, M., Meng, L., and Natarajan, R. Epigenetic histone H3 lysine 9 methylation in metabolic memory and inflammatory phenotype of vascular smooth muscle cells in diabetes. Proc Natl Acad Sci U S A **105,** 9047, 2008.
29. Clifford, R.L., John, A.E., Brightling, C.E., and Knox, A.J. Abnormal histone methylation is responsible for increased vascular endothelial growth factor 165a secretion from airway smooth muscle cells in asthma. J Immunol **189,** 819, 2012.
30. Ye, L., Fan, Z., Yu, B., Chang, J., Al Hezaimi, K., Zhou, X., *et al.* Histone demethylases KDM4B and KDM6B promotes osteogenic differentiation of human MSCs. Cell Stem Cell **11,** 50, 2012.
31. Eslaminejad, M.B., Fani, N., and Shahhoseini, M. Epigenetic regulation of osteogenic and chondrogenic differentiation of mesenchymal stem cells in culture. Cell J **15,** 1, 2013.
32. Musumeci, G., Castrogiovanni, P., Loreto, C., Castorina, S., Pichler, K., and Weinberg, A.M. Post-traumatic caspase-3 expression in the adjacent areas of growth plate injury site: a morphological study. Int J Mol Sci **14,** 15767, 2013.
33. Yao, Y., Wang, G., Wang, Z., Wang, C., Zhang, H., and Liu, C. Synergistic enhancement of new bone formation by recombinant human bone morphogenetic protein-2 and osteoprotegerin in trans-sutural distraction osteogenesis: a pilot study in dogs. J Oral Maxillofac Surg **69,** e446, 2011.
34. Song, G., Habibovic, P., Bao, C., Hu, J., van Blitterswijk, C.A., Yuan, H., *et al.* The homing of bone marrow MSCs to non-osseous sites for ectopic bone formation induced by osteoinductive calcium phosphate. Biomaterials **34,** 2167, 2013.
35. Lim, C.T., Ren, X., Afizah, M.H., Tarigan-Panjaitan, S., Yang, Z., Wu, Y., *et al.* Repair of osteochondral defects with rehydrated freeze-dried oligo[poly(ethylene glycol) fumarate] hydrogels seeded with bone marrow mesenchymal stem cells in a porcine model. Tissue Eng Part A **19,** 1852, 2013.
36. Kasten, P., Beverungen, M., Lorenz, H., Wieland, J., Fehr, M., and Geiger, F. Comparison of platelet-rich plasma and VEGF-transfected mesenchymal stem cells on vascularization and bone formation in a critical-size bone defect. Cells Tissues Organs **196,** 523, 2012.
37. Wang, Y., Mostafa, N.Z., Hsu, C.Y., Rose, L., Kucharki, C., Yan, J., *et al.* Modification of human BMSC with nanoparticles of polymeric biomaterials and plasmid DNA for BMP-2 secretion. J Surg Res **183,** 8, 2013.
38. Yan, S.G., Zhang, J., Tu, Q.S., Ye, J.H., Luo, E., Schuler, M., *et al.* Enhanced osseointegration of titanium implant through the local delivery of transcription factor SATB2. Biomaterials **32,** 8676, 2011.
39. Gyorgy, A.B., Szemes, M., de Juan Romero, C., Tarabykin, V., and Agoston, D.V. SATB2 interacts with chromatin-remodeling molecules in differentiating cortical neurons. Eur J Neurosci **27,** 865, 2008.
40. Jenuwein, T., and Allis, C.D. Translating the histone code. Science **293,** 1074, 2001.
41. Kouzarides, T. Chromatin modifications and their function. Cell **128,** 693, 2007.
42. Pinheiro, I., Margueron, R., Shukeir, N., Eisold, M., Fritzsch, C., Richter, F.M., *et al.* Prdm3 and Prdm16 are H3K9me1 methyltransferases required for mammalian heterochromatin integrity. Cell **150,** 948, 2012.
43. Petite, H., Viateau, V., Bensaid, W., Meunier, A., de Pollak, C., Bourguignon, M., *et al.* Tissue-engineered bone regeneration. Nat Biotechnol **18,** 959, 2000.
44. Wang, Y., Kim, H.J., Vunjak-Novakovic, G., and Kaplan, D.L. Stem cell-based tissue engineering with silk biomaterials. Biomaterials **27,** 6064, 2006.

Address correspondence to:
Jake Chen, DMD, PhD
Division of Oral Biology
Tufts University School of Dental Medicine
1 Kneeland Street
DHS-643
Boston, MA 02111

E-mail: jk.chen@tufts.edu

Qisheng Tu, MD, PhD
Division of Oral Biology
Tufts University School of Dental Medicine
1 Kneeland Street
DHS-638
Boston, MA 02111

E-mail: qisheng.tu@tufts.edu

Received: August 12, 2014
Accepted: April 2, 2015
Online Publication Date: June 8, 2015